Title	Micro-stepping control of ultrasonic stepping motors
Author(s)	Chau, KT; Shi, B; Hu, MQ; Jing, L; Fan, Y
Citation	Conference Record - Ias Annual Meeting (Ieee Industry Applications Society), 2004, v. 1, p. 353-359
Issued Date	2004
URL	http://hdl.handle.net/10722/54044
Rights	Creative Commons: Attribution 3.0 Hong Kong License

Micro-Stepping Control of Ultrasonic Stepping Motors

K.T. Chau, Bin Shi
Department of Electrical and Electronic Engineering
The University of Hong Kong
Hong Kong, China
ktchau@eee.hku.hk

Min-Qiang Hu, Long Jing, Ying Fan
Department of Electrical Engineering
Southeast University
Nanjing, China

***Abstract*—The ultrasonic stepping motor (USSM) using spatially shifted standing vibrations shows the advantages of high torque, good controllability and open-loop operation. Due to the segmentation problem of piezoelectric materials, the corresponding step size is practically limited. The purpose of this paper is to propose and implement micro-stepping control of this USSM. Different from the available half-step operation, the proposed control simultaneously varies both the combination of phase excitations and the magnitude of applied voltages in such a way that the desired step size can be attained. Digital implementation and experimental verification are given to validate the proposed micro-stepping control.**

Keywords-motor control; piezoelectric; stepping motor; ultrasonic motor

I. INTRODUCTION

The traveling-wave ultrasonic motor (TWUSM) has become attractive for servomechanism, since it offers the distinct advantages of high torque density, lightweight, compact size, fast response, no electromagnetic interference (EMI), quiet operation and power-down holding torque capability [1]-[3]. Nevertheless, the TWUSM still suffers from the drawback of closed-loop operation, thus desiring precision sensing devices [4], [5]. In order to get rid of this bulky and costly closed-loop system, the first ultrasonic stepping motor (USSM) was proposed in 1993 [6]. However, this motor generally involves many projections on the stator and many slits in the rotor, hence suffering from the difficulty in controlling the degenerated modes [7], [8].

Recently, a viable USSM using spatially shifted standing vibrations has been proposed in which the stator does not have any projections [9]. This motor shows the definite advantages of high torque, good controllability and open-loop operation. However, due to the segmentation problem of piezoelectric materials which are usually made of lead zirconate titanate (PZT), the corresponding step size or the number of steps per revolution is practically limited. Very recently, an attempt has been made to improve the step size of this USSM by borrowing the half-step operation of the conventional electromagnetic stepping motor [10].

Following the spirit of [10], the purpose of this paper is to propose and implement the micro-stepping control of the USSM using the principle of spatially shifted standing vibrations. Different from the previous half-step operation which successively conducts single-phase-on and two-phase-on excitation modes, the proposed micro-stepping control simultaneously varies both the combination of phase excitations and the magnitude of excitations in such a way that the desired step size can be attained. Different from the micro-stepping control of electromagnetic stepping motors in which the phase currents are modulated [11], the proposed micro-stepping control is to modulate the applied phase voltages.

In Section II, the operating principle of the USSM using spatially shifted standing vibrations will be briefly described. Then, the newly proposed micro-stepping control of this USSM will be discussed in Section III. Section IV will be devoted to present the implementation of the whole system. In Section V, experimental characteristics of the prototype will be given to verify the proposed micro-stepping operation. Finally, conclusions will be drawn in Section VI.

II. PRINCIPLE OF OPERATION

The configuration of the USSM using spatially shifted standing vibrations is depicted in Fig. 1. It is an 80-step (N=80) USSM with the order of vibration mode n=8, the number of spatial phase shifts (which is equivalent to the number of driving phases) p=5, the number of electrode divisions q=20 and the number of sections m=4 to excite a mode each time. The rotor consists of 16 blades machined at the contact surface with the stator.

Fig. 2 shows the principle of stepping of the USSM. When the electrodes of phase A are fed by the applied voltage, the standing-wave vibration is excited. Then, the force F is applied to the rotor by the flexural bending vibration of the stator. The corresponding horizontal component F_x pushes the rotor moving to the nodal line position of the stator. By exciting the phases in sequence, the nodal line moves along the circumference of the stator. Thus, the rotor moves with the nodal line. The sequence of excitation is shown in Table I.

The design criteria and design procedure of this USSM have been discussed in [12]. In this paper, the normal operation (namely, the small step size operation) of the USSM is considered, whereas the abnormal operation (namely, the large step size operation) is ignored. In short, the design parameters are governed by [12]:

This work was supported and funded by a grant from Research Grants Council of Hong Kong Special Administrative Region, China.

$$q = \frac{2nN}{N-2n} \tag{1}$$

$$p = \frac{N}{2n} \tag{2}$$

$$m = \frac{q}{p} \tag{3}$$

In order to determine the driving frequency to excite the desired vibration mode, a vibration analysis is conducted. In general, a commercially available finite element method (FEM) software package can be utilized. The analysis result is shown in Fig. 3, in which the B_{08} vibration mode is adopted. Hence, the resonant frequency can be calculated as 44.9 kHz.

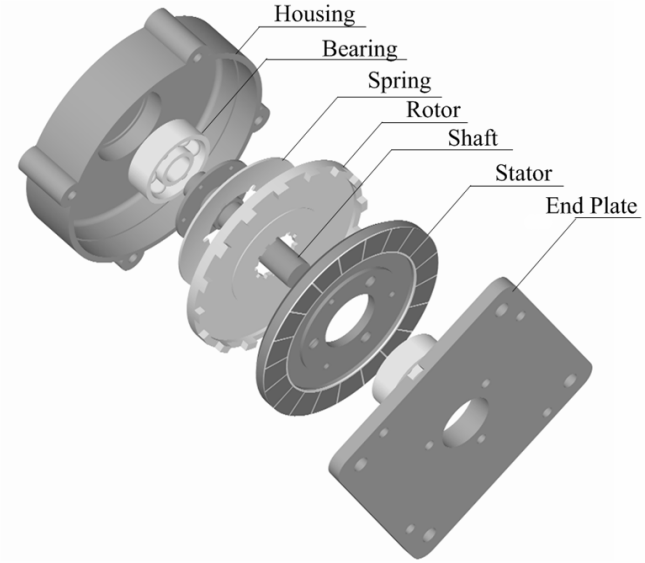

Figure 1. USSM configuration.

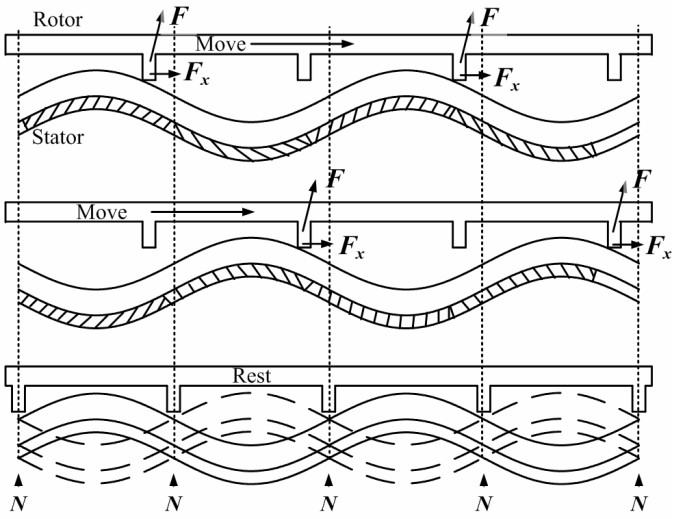

Figure 2. Principle of stepping.

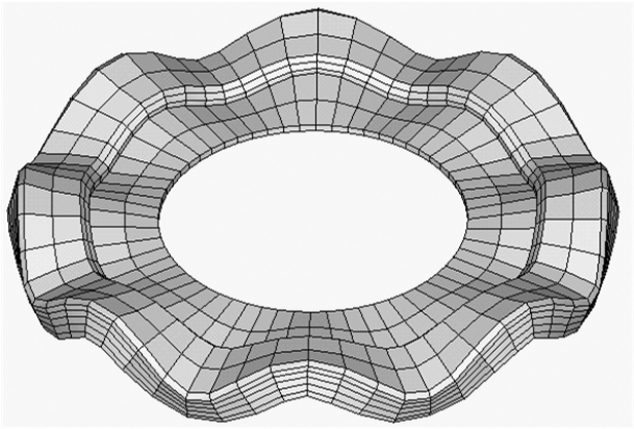

Figure 3. FEM simulated vibration pattern.

TABLE I. EXCITATION SEQUENCE OF FULL-STEP OPERATION

	1	2	3	4	5
A	X				
B		X			
C			X		
D				X	
E					X

III. MICRO-STEPPING CONTROL

In order to illustrate the proposed micro-stepping control approach, three typical fractional-step operations (namely the half-step, one-third-step and two-third-step operations) are graphically depicted. Notice that the number of micro-steps can be flexibly controlled to achieve different fractional steps. Theoretically, the size of these micro-steps is unconstrained; however, its size is practically limited by the physical tolerances and manufacturing imperfections of the USSM during prototyping.

Fig. 4(a) shows the concept of half-step operation. The corresponding movement equals half of one step, so-called the half-step operation. The corresponding excitation sequence is shown in Table II. Extending this concept, the adjustment of both the combination of phase excitations and the magnitude of applied voltages can further subdivide the original step size.

The steps from Phase A to Phase B are adopted for exemplification. When phase A and phase B are excited, the spatial displacement distribution of the vibration can be expressed as:

$$f_a = A\sin n\theta, \tag{4}$$

$$f_b = B\sin n(\theta - \theta_s), \tag{5}$$

where $\theta_s = 2\pi / N$ denotes the spatial distance between phase A and phase B, and A and B denote the corresponding vibration amplitudes. When phase A and phase B are excited simultaneously, the spatial displacement distribution can be expressed as:

$$f_{ab} = f_a + f_b . \tag{6}$$

Substituting (4) and (5) into (6), it yields:

$$f_{ab} = F_{ab} \sin n(\theta - \varphi), \tag{7}$$

where the corresponding amplitude and phase difference are given by:

$$F_{ab} = \sqrt{(A + B\cos n\theta_s)^2 + (B\sin n\theta_s)^2}\ , \tag{8}$$

$$\varphi = \frac{1}{n}\arctan\left(\frac{(B/A)\sin n\theta_s}{1+(B/A)\cos n\theta_s}\right). \tag{9}$$

Thus, when the excitation switches from phase A to the simultaneous excitation of both phase A and phase B, the micro-step angle θ_μ is equal to the angle shift from the initial nodal line (the zero-crossing point of f_a) to the new nodal line (the zero-crossing point of f_{ab}). Hence, it yields:

$$\theta_\mu = \varphi . \tag{10}$$

Substituting (9) into (10), θ_μ can be expressed as:

$$\theta_\mu = \frac{1}{n}\arctan\left(\frac{(B/A)\sin n\theta_s}{1+(B/A)\cos n\theta_s}\right). \tag{11}$$

After rearrangement, the voltage amplitude ratio (B/A) can be expressed in terms of θ_μ as given by:

$$(B/A) = \frac{\tan n\theta_\mu}{\sin n\theta_s - \tan n\theta_\mu \cos n\theta_s}\ . \tag{12}$$

It indicates that once the micro-step size is given, there is an appropriate voltage amplitude ratio. Fig. 4 illustrates the realization of the 50%-step (half-step), 33%-step (one-third-step) and 67%-step (two-third-step) of the USSM when the values of (B/A) are chosen as 1, 0.5 and 2, respectively. The corresponding excitation sequences are tabulated in Table II, Table III and Table IV, respectively.

From Table II and Table III, the numbers of micro-steps within a full-step are 2 and 3, respectively. Since they are both integers, the excitation sequences are repeated after each cycle. On the other hand, from Table IV, the number of micro-steps within a full-step is 3/2 so that the excitation sequence can only be repeated after two cycles. Of course, an integer multiple of micro-steps within a full-step is preferred.

By using (11), when n = 8 and θ_s=4.5°, the relationship between θ_μ and (B/A) is plotted in Fig. 5 which can provide the designer an easy tool to select number of micro-steps and the desired applied voltage amplitudes. It can be seen that the lower the (B/A) is selected, the smaller the θ_μ and hence the larger the number of micro-steps are resulted.

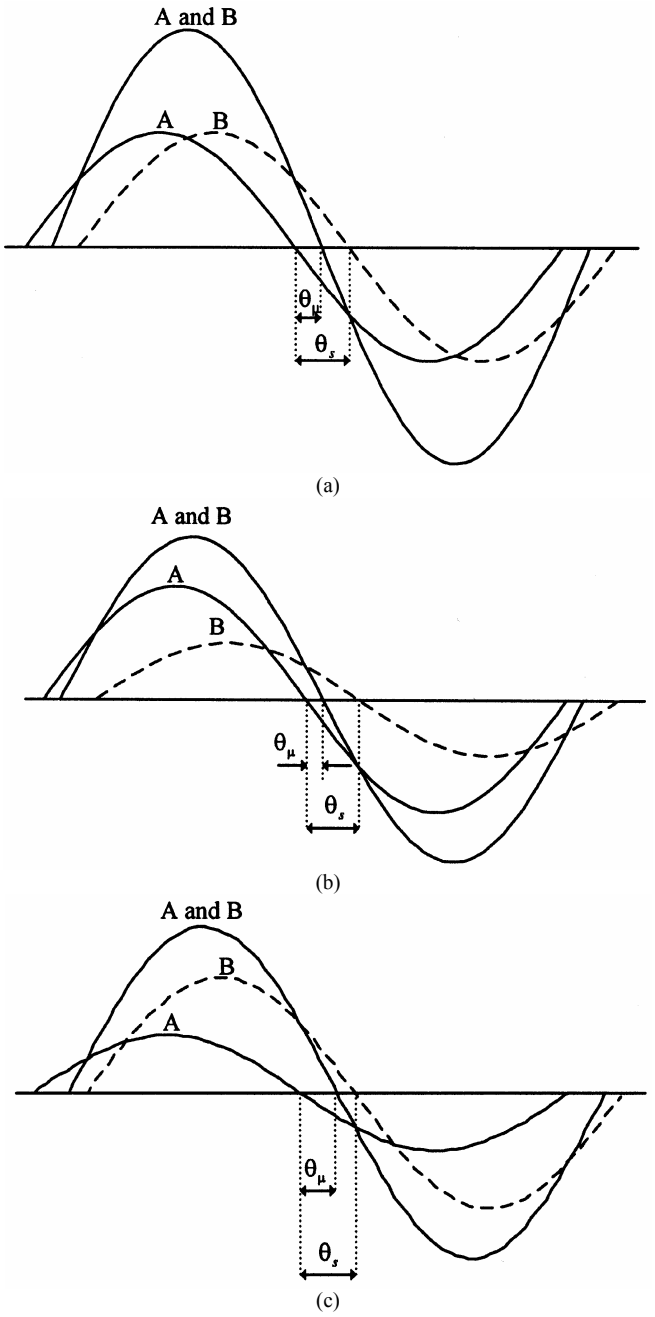

Figure 4. Principle of micro-step operations. (a) 50%-step. (b) 33%-step. (c) 67%-step.

TABLE II. EXCITATION SEQUENCE OF 50%-STEP OPERATION

	1	2	3	4	5	6	7	8	9	10
A	X	X								X
B		X	X	X						
C				X	X	X				
D						X	X	X		
E								X	X	X

TABLE III. EXCITATION SEQUENCE OF 33%-STEP OPERATION

	1	2	3	4	5	6	7	8	9	10	11	12	13	14	15
A	X	X	X											X	X
B		X	X	X	X	X									
C					X	X	X	X	X						
D								X	X	X	X	X			
E											X	X	X	X	X

EXCITATION SEQUENCE OF 67%-STEP OPERATION

	1	2	3	4	5	6	7	8	9	10	11	12	13	14	15
A	X	X													X
B		X	X												
C			X	X	X										
D					X	X									
E						X	X	X							
A								X	X						
B									X	X	X				
C											X	X			
D												X	X	X	
E														X	X

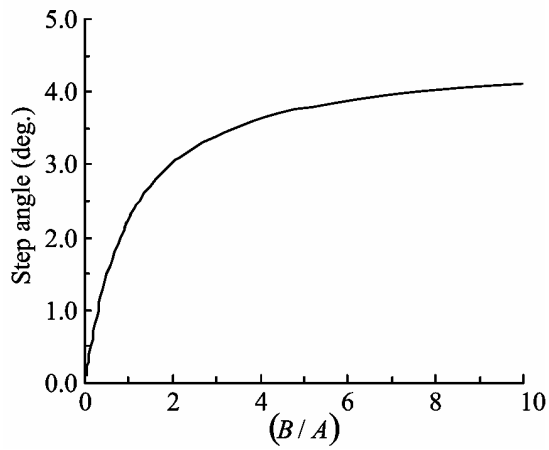

Figure 5. Micro-step angle versus voltage amplitude ratio.

IV. IMPLEMENTATION

The USSM configuration shown in Fig. 1, namely n=8, q=20, p=5 and m=4, is prototyped. The corresponding structure is shown in Fig. 6. Since the elastic modulus of phosphor bronze is insensitive to the varying temperature, it is selected as the material of the elastic ring of the stator. The rotor is made of aluminum because of its lightweight and easy machining. The physical and geometric parameters of this prototype are tabulated in Table V and Table VI, respectively.

To implement the micro-stepping movement, the control and driving circuit block diagram shown in Fig. 7 is used. The hardware core is the low-cost TMS320F240 microcontroller which offers the calculation of (B/A) for a given θ_μ or the number of micro-steps, the output interfaces for generating control signals, as well as the input interfaces for receiving command and measured data. The motion command can be any pattern of stepping motions with the direction governed by the clockwise/counterclockwise (CW/CCW) control unit. The ultrasonic driving frequency is generated by a voltage controlled oscillator (VCO) unit. The variable voltage control unit is to generate the applied voltages based on the calculated (B/A). After feeding the switching control signals and driving frequency into the logic control unit, the desired logic control signals are resulted. Then, these logic control signals and the variable voltage control signal are amplified to drive the USSM. It should be noted that the whole system is under open-loop operation. The encoder and hence the measured position and speed data are used for display only. Fig. 8 shows the prototype of this control and driving circuit.

Fig. 9 shows the test-bed of the prototype for evaluation. A DC servo motor is coupled to the USSM and works as the dynamometer. The load torque of this test-bed can be flexibly controlled by electrically connecting a programmable electronic load to this DC servo motor.

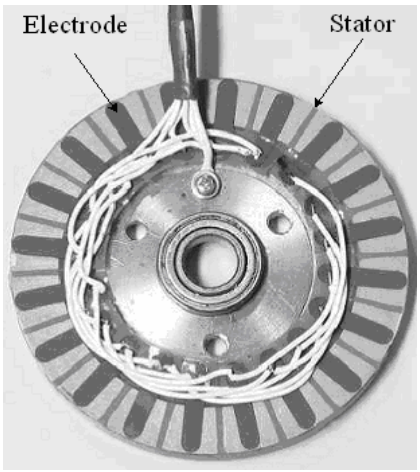

(a)

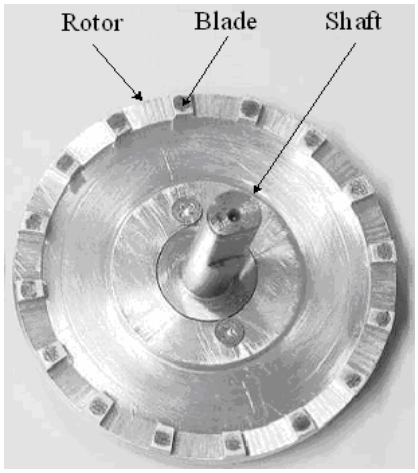

(b)

Figure 6. USSM prototype. (a) Stator with 20 electrodes. (b) Rotor with 16 blades.

TABLE IV. PHYSICAL PARAMETERS OF PROTOTYPE

Initial number of steps	80
Initial step size	4.5°
Order of vibration mode	8
Number of driving phases	5
Number of electrodes	20
Number of blades	16

TABLE V. GEOMETRIC PARAMETERS OF PROTOTYPE

Inner radius of stator	22.5 mm
Outer radius of stator	30.0 mm
Height of stator	3.0 mm
Height of electrodes	0.5 mm
Inner radius of rotor	26.0 mm
Outer radius of rotor	29.0 mm
Height of rotor	3.0 mm
Circumferential width of blades	2.8 mm
Radial width of blades	3.0 mm
Height of blades	1.8 mm
Radius of shaft	4.0 mm
Height of shaft	36.0 mm

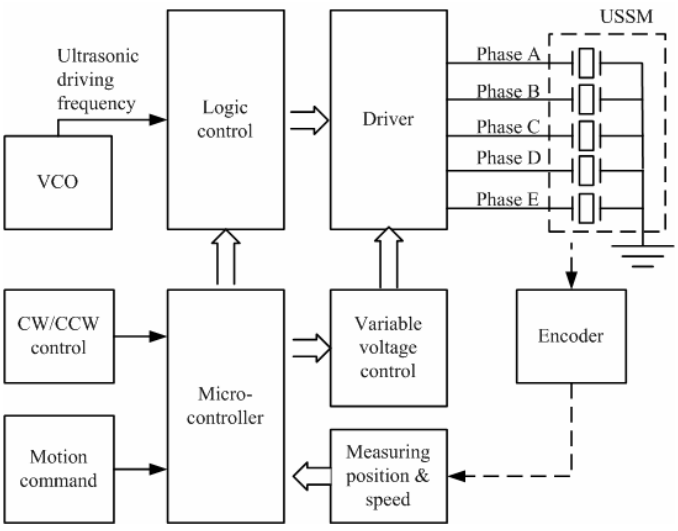

Figure 7. Control and driving circuit block diagram.

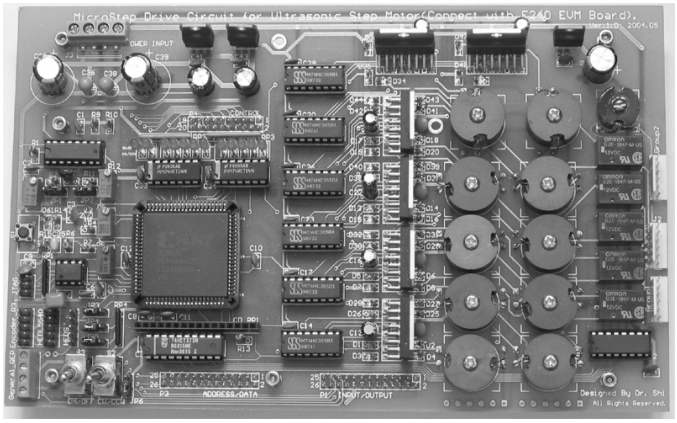

Figure 8. Control and driving circuit protype.

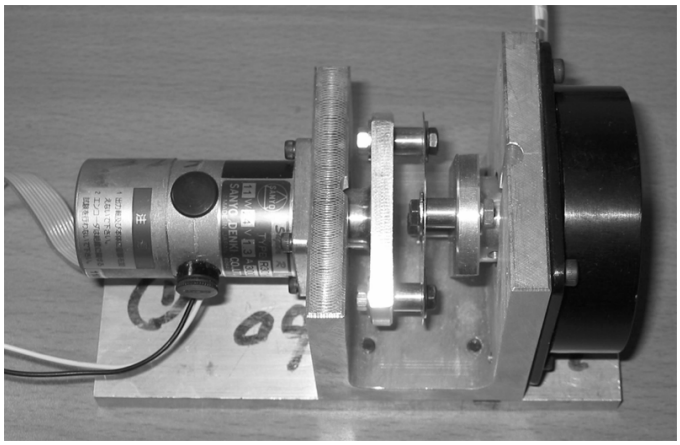

Figure 9. Test-bed of prototype.

V. EXPERIMENTAL CHARACTERISTICS

Firstly, the vibration mode, namely B_{08}, is experimentally verified by using a laser Doppler vibrometer. Fig. 10 shows the measured spatial distribution of the vibration when the phase A is excited, which agrees with the FEM simulated vibration pattern shown in Fig. 3.

Secondly, the dynamic characteristics of the proposed micro-stepping control approach for the USSM are investigated. Two integer multiples of micro-steps, namely the 50%-step and 33%-step operations, are implemented. Fig. 11 shows the position response for a command of five forward steps when micro-stepping control is activated for 50%-step operation. Similarly, the position response under 33%-step operation is shown in Fig. 12. It is obvious that the measured responses well verify the accuracy of micro-step angles (2.25° for 50%-step operation and 1.5° for 33%-step operation).

Finally, the transient performances of the proposed approach for the USSM are investigated. A step command is adopted for illustration. Fig. 13 and Fig. 14 show the measured transient position and speed responses at different load torques, respectively. It can be found that the response times are all less than 80 ms, confirming that the USSM can offer excellent transient performances.

Figure 10. Measured vibration pattern using laser Doppler vibrometer.

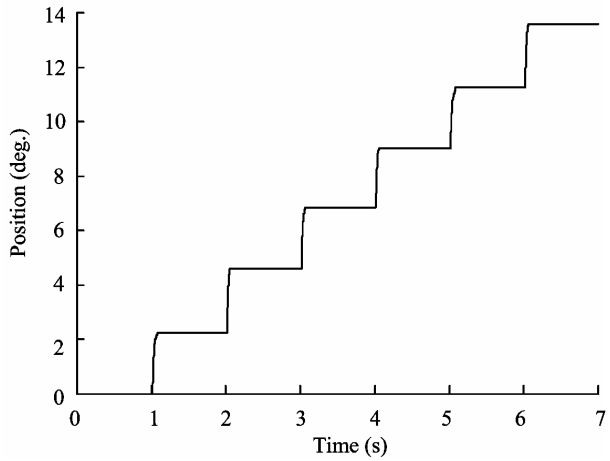

Figure 11. Measured position response under 50%-step operation for a command of 5 forward steps.

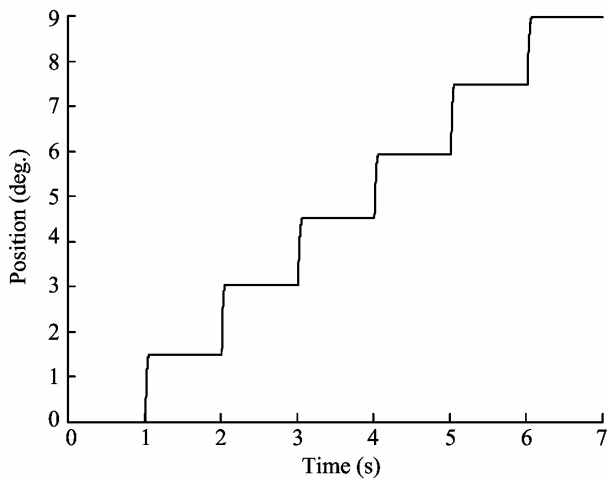

Figure 12. Measured position response under 33%-step operation for a command of 5 forward steps.

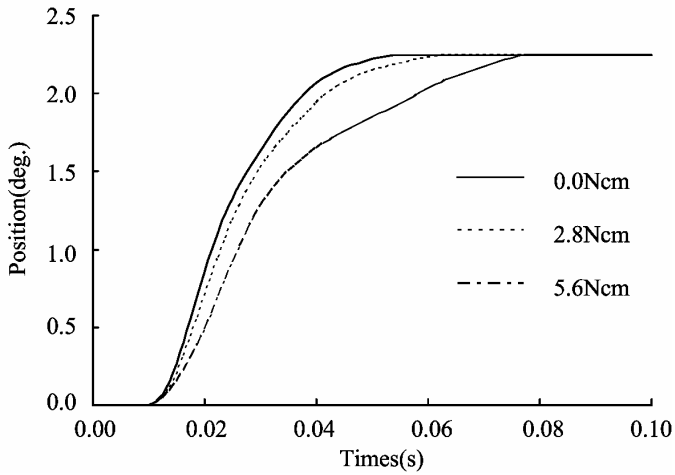

Figure 13. Measured transient position response under 50%-step operation at different loads.

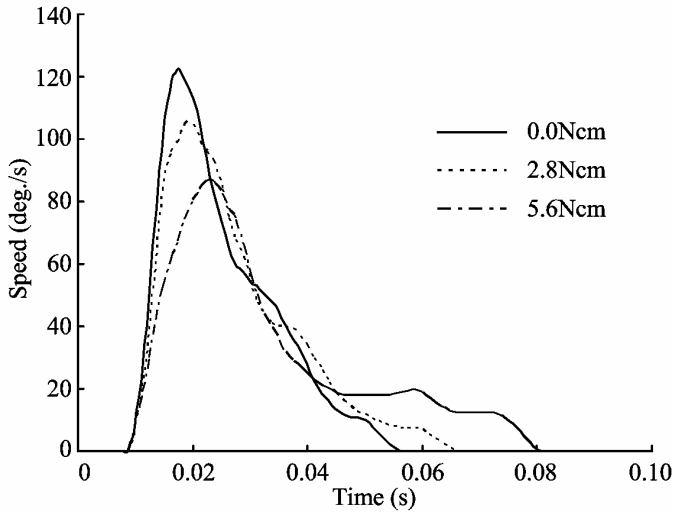

Figure 14. Measured transient speed response under 50%-step operation at different loads.

VI. CONCLUSIONS

In this paper, a new micro-stepping control approach has been proposed and implemented for the USSM using spatially shifted standing vibrations. The key is to simultaneously adjust both the combination of phase excitations and the corresponding voltage amplitude ratio in such a way that the desired step size can be attained. Digital implementation and experimental characteristics of the USSM at the 50%-step and 33%-step operations are given to verify the proposed micro-stepping control.

REFERENCES

[1] T. Sashida, and T. Kenjo, *An Introduction to Ultrasonic Motors*. New York: Oxford Science Publications, 1993.

[2] S. Ueha, and Y. Tomikawa, *Ultrasonic motors: Theory and Applications*. New York: Oxford Science Publications, 1993.

[3] K. Uchino, "Piezoelectric ultrasonic motors: overview," *Smart Materials and Structures*, Vol. 7, No. 3, 1998, pp. 273-285.

[4] K.T. Chau, and S.W. Chung, "Servo position control of ultrasonic motors using fuzzy neural network," *Electric Machines and Power Systems*, Vol. 29, No. 3, 2001, pp. 229-246.

[5] K.T. Chau, and S.W. Chung, "Servo speed control of traveling-wave ultrasonic motors using pulse width modulation," *Electric Power Components and Systems*, Vol. 29, No. 8, 2001, pp. 707-722.

[6] X. Chen, C. Kusakabe, Y. Tomikawa, and T. Takano, "Rotor displacement of the ultrasonic motor having an angular displacement self-correction function," *Japanese Journal of Applied Physics*, Vol. 32, Part 1, No. 9B, 1993, pp. 4198-4201.

[7] C. Kusakabe, "Effect of pressing force applied to a rotor on disk-type ultrasonic motor driven by self-oscillation," *Japanese Journal of Applied Physics*, Vol. 37, Part 1, No. 5B, 1998, pp. 2966-2969.

[8] S. He, W. Chen, X. Tao, and Z. Chen, "Standing wave bi-directional linearly moving ultrasonic motor," *IEEE Transactions on Ultrasonics, Ferroelectrics and Frequency Control*, Vol. 45, 1998, pp. 1133-1139.

[9] K. Nakamura, J. Margairaz, T. Ishii, and S. Ueha, "Ultrasonic stepping motor using spatially shifted standing vibrations," *IEEE Transactions on Ultrasonics, Ferroelectrics and Frequency Control*, Vol. 44, No. 4, 1997, pp. 823-827.

[10] K.T. Chau, B. Shi, and M.Q. Hu, "A design method and half-step operation for ultrasonic stepping motors," *IEEE Transactions on Industry Applications*, Vol. 39, No. 4, 2003, pp. 953-960.

[11] D. Xu, and Y. Jiang, "A method and implementation of fully digitized continuous microstep for step motor," *IEEE International Electric Machines and Drives Conference*, 1997, pp. TC2/9.1-TC2/9.3.

[12] K.T. Chau, B. Shi, M.Q. Hu, and S.W. Chung, "Design and control of a new ultrasonic stepping motor," *IEEE Industry Applications Conference*, 2002, pp. 2259-2266.